May 2026

The Chirality-Flow Formalism in Charged Current Weak Interactions

Victor Hallberg

Theoretical Particle Physics
Department of Physics
Lund University

Bachelor thesis (15 hp, project duration: 2 months) supervised by Malin Sjödahl

Abstract

The chirality-flow formalism is an extension of the spinor-helicity formalism in which scattering amplitudes are represented as diagrams of oriented flow lines between external spinors, which allows spinor bracket products to be read off easily. While the formalism has been explored and implemented for Quantum Electrodynamics (QED) and Quantum Chromodynamics (QCD) interactions, its application has not been explored systematically in the full electroweak sector.

This thesis investigates the application of the chirality-flow formalism to charged current weak interactions. Since the the W boson is fundamentally chiral, only coupling to left-handed fermions, it proves to yield simplifications beyond those present in QED and QCD. We show that the amount of diagrams produced reduces by one fourth compared to equivalent interactions, imposing a "lock" on the chiral flow. Furthermore, the treatment of external W bosons demonstrates how the choice of reference vector eliminates one of the transverse polarization vectors. Finally, it is shown how the lock on chirality-flow propagates through massless fermion lines, constraining subsequent vertices of other interaction types.

Contents

Acronyms

QCD Quantum Chromodynamics.

QED Quantum Electrodynamics.

1 Introduction

The standard model of particle physics represents one of the most successful theoretical frameworks in the history of science, describing three of four fundamental forces and the elementary particles that make up all known matter in the universe [1]. From the standard model Lagrangian we are able to derive scattering amplitudes, which are complex valued numbers, typically denoted $\mathcal{M}$, which yield the transition probabilities between initial and final states. They are therefore a necessary quantity to calculate cross sections and decay rates. However, the calculation of these probabilities become increasingly complex as the number of external particles increases. To counter this, the need for efficient methods of calculating scattering probabilities becomes increasingly clear.

The traditional, and perhaps most well-known, method for computing scattering is through the use of Feynman diagrams [1]. Whilst this method is systematic and physically transparent, it quickly becomes algebraically unwieldy as the number of particles and interaction vertices increases. Typical methods end up with terms growing as factorials for higher multiplicity interactions [2]. Even quite simple processes can become rather expansive algebraically during intermediary stages due to trace expansion, even if the final result is compact.

One tool to ease with the complexity of scattering calculations, especially in the massless case, is the spinor-helicity formalism, which reformulates scattering amplitudes in terms of two-component Weyl spinors associated with helicity states [2]. Rather than working with four-vectors and gamma matrices, this approach exploits the isomorphism between the Lorentz group and SL(2,C) to express amplitudes as products of spinor brackets:

$$\Psi = \begin{pmatrix} |a] \\ |b\rangle \end{pmatrix}, \overline{\Psi} = \Psi^\dagger \gamma^0 = ([b|, \langle a|),$$

where $|b]$ and $|a\rangle$ are left- and right-chiral Weyl spinors, as are given in section 2.3. The resulting expressions are remarkably compact. (An explicit example in of this can be found in [3]).

Building on the spinor-helicity formalism, the chirality-flow formalism was introduced as a way of making it immediately transparent which spinor inner products vanish by using chirality[4]. In this formalism, amplitudes can be represented as diagrams displaying the flow of fermions and chirality along lines connecting external spinors. This is doubly beneficial, as it both makes calculations more compact as well as more transparent, since the main structure of the amplitude is already revealed before any algebra is performed.

The chirality-flow formalism has so far primarily been explored and implemented for QED and QCD [5]. However, it has not been explored and understood as well in the context of electroweak interactions, which are inherently chiral in nature, exhibiting the maximal parity violation $(1 - \gamma^5)$ at every weak vertex [6]. This implies that a large fraction of helicity configurations vanish identically in any charged-current process. In the spinor-helicity and chirality-flow languages, this should translate into dramatic simplifications, beyond those seen in QCD and QED.

The goal of this thesis is to investigate how the chirality-flow formalism can be consistently and meaningfully applied to charged current weak interactions, and to characterize the simplifications that the chiral nature of the weak force introduces. We begin with the massless limit of fermion-fermion scattering via W exchange, where the formalism takes its simplest form, before extending the treatment to include fermion mass effects. The polarization structure of the external W boson is then examined. Throughout, results are compared with standard Feynman diagram calculations, to make simplifications concrete and quantitative.

The thesis is structured as follows. In section 2 we introduce the theoretical background necessary for understanding and following the calculations that proceed it. Following that, section 3 presents the simplest charged current process, and treating it first in the massless limit and then in the massive case. Further, section 4 treats the decay of an on-shell external W boson and examines reference vector choices. Afterward, section 5 examines whether the simplifications established in previous sections persist when the number of external particles is increased. Finally, section 6 presents the conclusion, and section 7 presents an outlook for future work.

2 Background

2.1 Scattering Amplitudes and Helicity

In quantum field theory, scattering interactions are described by transition amplitudes between initial and final states. These amplitudes are encoded in the S-matrix, which relate the free particle states. For a certain transition between an initial state $|i\rangle$ and final state $|f\rangle$, the S-matrix element can be written as

$$S_{fi} = \langle f|S|i\rangle. \tag{2.1}$$

For a certain process the scattering amplitude $\mathcal{M}$ is extracted from the S-matrix element by factoring out a momentum-conserving delta function:

$$\langle f|S|i\rangle = (2\pi)^4 \delta^{(4)}(p_f - p_i) \cdot i\mathcal{M}. \tag{2.2}$$

The physical observables are then obtained from $|\mathcal{M}|^2$ by integrating over an appropriate phase space.

A key choice in any amplitude calculation is how to treat the spin degrees of freedom of the external particles, for which an efficient approach is to work with external particle states of definite helicity. Helicity is defined as particle spin projected along the direction of motion:

$$h = \hat{p} \cdot \vec{J}. \tag{2.3}$$

For massless particles, this is a Lorentz-invariant quantity, making it a useful quantum number for labelling external states in a massless case. This differs from the massive case as you are able to boost the particle such that the momentum direction flips relative to the spin.

2.2 Weyl Spinors and Chirality

In the chiral, or Weyl, representation of a Dirac ψ spinor, the four-component object is decomposed into two two-component Weyl spinors

$$\psi = \begin{pmatrix} \psi_L \\ \psi_R \end{pmatrix}, \tag{2.4}$$

where ψ_L and ψ_R are left- and right-handed chiral components, defined as eigenstates of the chirality operator γ^5 [1].

In the massless limit these two spinors decouple completely, and chirality is one-to-one with helicity. In the massive case however, the Dirac Lagrangian mixes the spinors so that this is no longer the case. Fermion helicity thus becomes a superposition of both chiral components. A definite chirality can be determined using the left-, P_L, and right-, P_R, handed chiral projection operators, defined as

$$P_L = \frac{1-\gamma^5}{2},$$

$$P_R = \frac{1+\gamma^5}{2}.$$

2.3 The Spinor-Helicity Formalism

The spinor-helicity formalism utilises the observation that the momentum of a massless particle can be written as the product of Weyl spinors [2]. For a massless four-momentum p^μ, where $p^2 = 0$, one can write the relevant bispinor as

$$p_{\alpha\dot{\alpha}} = p_\mu \sigma^\mu_{\alpha\dot{\alpha}} = \lambda_\alpha \tilde{\lambda}_{\dot{\alpha}} \tag{2.5}$$

where $\sigma^\mu_{\alpha\dot{\alpha}}$ is the Pauli-sigma matrix, and the resulting matrix $p_{\alpha\dot{\alpha}}$ factorizes into λ_α and $\tilde{\lambda}_{\dot{\alpha}}$, which represent the right- and left-handed Weyl spinors respectively. The dotted and undotted indices are raised and lowered using the two-dimensional levi-civita tensors $\epsilon^{\alpha\beta}$ and $\epsilon_{\alpha\beta}$. These are defined as $\epsilon^{12} = \epsilon_{21} = 1$ and $\epsilon^{21} = \epsilon_{12} = -1$ (and identically for dotted indices), such that

$$\lambda^\alpha = \epsilon^{\alpha\beta}\lambda_\beta, \qquad \lambda_\alpha = \epsilon_{\alpha\beta}\lambda^\beta. \tag{2.6}$$

From these spinors one can construct the Lorentz-invariant inner products, the spinor brackets

$$\langle ij \rangle = \lambda_i^\alpha \lambda_{j,\alpha} \tag{2.7}$$

$$[ij] = \tilde{\lambda}_{i,\dot{\alpha}} \tilde{\lambda}_j^{\dot{\alpha}}. \tag{2.8}$$

These are antisymmetric such that $\langle ij \rangle = -\langle ji \rangle$ and $[ij] = -[ji]$, and connect to the Lorentz product corresponding to momenta by

$$\langle ij \rangle [ji] = 2p_i \cdot p_j = s_{ij}. \tag{2.9}$$

Furthermore, they fulfill the Schouten identity [7],

$$\langle ij\rangle\langle kl\rangle + \langle ik\rangle\langle lj\rangle + \langle il\rangle\langle jk\rangle = 0, \tag{2.10}$$

(identical for square brackets) which lets products of brackets be rearranged, and together with momentum conservation allows for the reduction of amplitudes to a minimal set of independent bracket products.

For outgoing particles there are four possible types of Weyl spinors for massless particles corresponding to the two fermion types along with chirality type [4]. They are (with Feynman diagrams on the left and chirality-flow diagrams on the right):

Right-chiral fermion, $\langle i| =$ 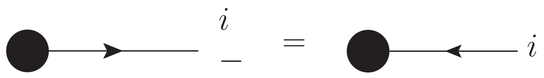

(2.11)

right-chiral anti-fermion, $|j\rangle =$ 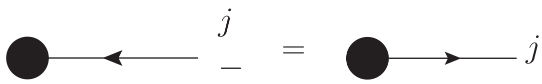

(2.12)

left-chiral fermion, $[i| =$ 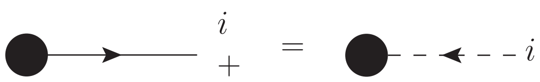

(2.13)

left-chiral anti-fermion, $|j] =$ 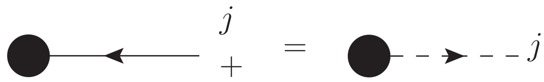

(2.14)

The label $\pm$ attached to the Feynman diagrams indicate whether the particle has negative or positive helicity. In the massless limit this is one-to-one with chirality. For the chirality-flow diagrams a dotted line represents left-chiral flow and a solid line represents right-chiral flow. The direction of the arrow in the chirality flow diagrams indicate the direction of the flow. This is distinct from the direction of the arrows in the Feynman diagram indicating fermion number flow.

Polarization vectors for gauge bosons are also able to be naturally represented by the spinor-helicity formalism, as will be shown in eqs. (2.23) to (2.25). Linking together two objects, we contract the Lorentz indices as

$\langle ij\rangle =$  , (2.15)

$[ij] =$ 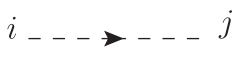 , (2.16)

with the undotted line representing right-chiral flow, and the dotted line representing left-chiral flow.

2.4 Chirality in Weak Interactions

The charged current interaction violates parity maximally, meaning that the left-handed projection operator will appear at every interaction vertex. This means that only the left-handed chiral component of a fermion field will interact with the charged current, and as such, right-handed fermions are essentially "blind" to W bosons.

For helicity amplitude calculations the fact that only left-chiral fermions interact with the W means that in the massless limit of the charged-current interaction, where chirality and helicity are one-to-one, any Feynman diagram involving right-chiral fermions at the W-vertex will vanish identically. As such, one can discard entire helicity configurations before carrying out any algebra.

For massive fermions the situation differs significantly. Since mass terms mix chirality eigenstates, a massive fermion of definite helicity is actually a superposition of left- and right-handed components. What this means is that for massive fermions, all helicity states will contribute.

2.5 The Chirality-Flow Formalism

The chirality-flow formalism was introduced as an extension of the spinor-helicity formalism, in which the amplitude is reorganised by grouping terms according to the flow of chirality through the diagram [4]. By expressing the algebra graphically one is able to read the spinor bracket products directly from the diagram.

In a Feynman diagram, each fermion line carries a chirality flow; A left-chiral flow line connects dotted spinor indices, contributing square brackets, and right-chiral flow lines connect undotted spinor indices, contributing angle brackets. The diagram is then constructed by tracing these flow lines between connected spinors, following propagators and vertices.

The rules can be summarised rather compactly: Massless fermion propagators contain a momentum matrix which flips the chirality-flow from left to right (and vice-versa). A vector boson vertex connects right-handed flow lines with left-handed ones, at the vertex of which the polarization vector of the gauge boson is inserted. Finally, external fermion states are represented by the spinors $|i\rangle$ and $|j]$ at the end points of the flow lines. The amplitude then simply becomes the product of all spinor-brackets formed by the connected flow lines.

For a massive incoming fermion with positive helicity we have

$$u(p) = \begin{pmatrix} -e^{-i\phi}\sqrt{\alpha}|q] \\ |p^\flat\rangle \end{pmatrix} =$$

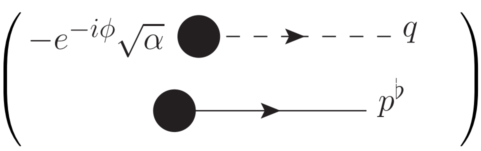

, (2.17)

and similarly for a massive incoming anti-fermion with positive helicity we have

$$\overline{v}(p) = \begin{pmatrix} |p^\flat] \\ -e^{i\phi}\sqrt{\alpha}|q\rangle \end{pmatrix} =$$ 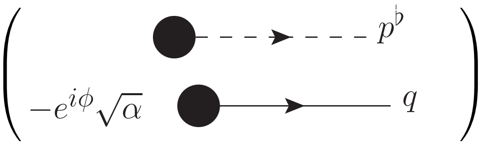

, (2.18)

where $p^\flat$ and q are two lightlike fourvectors satisfying $p^\flat \cdot q \neq 0$, and related to the massive fourvector p as

$$p = p^\flat + \alpha q \ , \text{ where } \alpha = \frac{p^2}{2p^\flat \cdot q}, \tag{2.19}$$

(other fermion species' are found in appendix A) [8]. From this decomposition it follows that the axis s^μ along which we measure the spin of a particle can be written:

$$s^\mu = \frac{1}{m}(p^{\flat\mu} - \alpha q^\mu). \tag{2.20}$$

For this we require that $s^2 = -1$ and $s \cdot p = 0$, making the arbitrary choice of reference vector physical, which leads to different spin amplitudes. For fermions there is also the fermion propagator (in both bra-ket and chirality-flow notation)

$$\frac{i}{p^2 - m^2}\begin{pmatrix} m & \not{p} \\ \bar{\not{p}} & m \end{pmatrix} = \frac{i}{p^2 - m^2}$$ 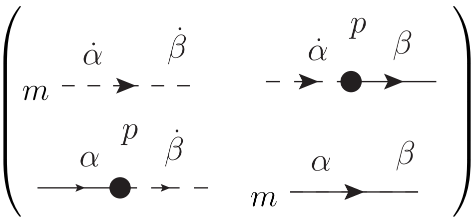

, (2.21)

where $\not{p} = |p^\flat]\langle p^\flat| + \alpha|q]\langle q|$. For the massless case $\alpha = 0$ (Note that this α is the one from eq. (2.19), not eq. (2.21)).

The vector propagator also contains a factor $\frac{i}{p^2 - m^2}$, however it is otherwise not similar:

$$-i\frac{g_{\mu\nu}}{p^2 - m^2} \Rightarrow -\frac{i}{p^2 - m^2}$$ 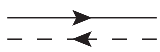 or $-\frac{i}{p^2 - m^2}$ 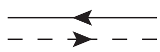 . (2.22)

We also need to define the polarisation vectors ϵ^μ_+, ϵ^μ_-, and ϵ^μ_0 as well as the fermion-vector boson vertex. The polarisation vectors are given as

$$\epsilon^\mu_L(p) = \frac{|p^\flat]\langle q|}{\langle q p^\flat\rangle} \text{ or } \frac{|q\rangle[p^\flat|}{\langle q p^\flat\rangle} = \frac{1}{\langle q p^\flat\rangle}$$ 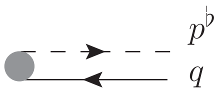

or $\frac{1}{\langle q p^\flat\rangle}$ 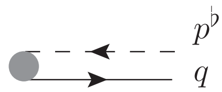

, (2.23)

$$\epsilon^\mu_R(p) = \frac{|q]\langle p^\flat|}{[p^\flat q]} \text{ or } \frac{|p^\flat\rangle[q|}{[p^\flat q]} = \frac{1}{[p^\flat q]}$$ 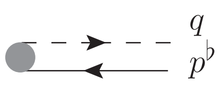

or $\frac{1}{[p^\flat q]}$ 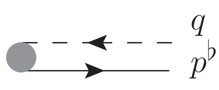

, (2.24)

$$\epsilon^\mu_0(p) = \frac{|p^\flat]\langle p^\flat| - \alpha|q]\langle q|}{m\sqrt{2}} = \frac{1}{m\sqrt{2}}$$ 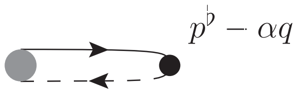

or $\frac{1}{m\sqrt{2}}$ 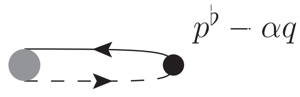

, (2.25)

where L corresponds to a left-helicity incoming $(-)$ or a right-helicity outgoing $(+)$ gauge boson, and vice versa for R (here, grey particle dots are used to differentiate them from the black momentum dots). Finally, the fermion-vector boson vertex is given as

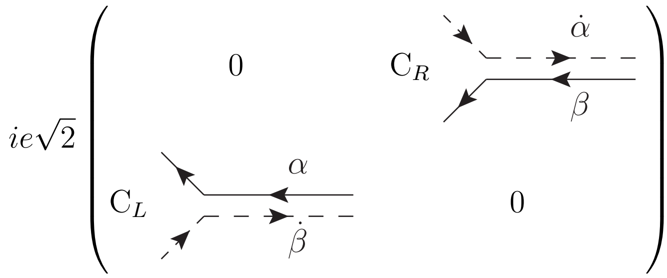

(2.26)

.

The application of this method to charged-current weak interactions, which is the subject of this thesis, demonstrates the full extent of these simplifications. Because the W boson couples exclusively through the left-handed projector, all charged current vertices impose a definite chirality on the fermion lines. It is this feature that makes the chirality-flow formalism particularly well suited to the electroweak case, and its consequences for scattering-amplitude calculations will be explored throughout the remainder of this thesis.

3 Fermion Scattering via W bosons

The simplest charged current scattering process is the annihilation and pair production of fermions via $W^{\pm}$. We label the external particle momenta p_1, p_2, p_3, and p_4 for the incoming and outgoing fermion and antifermion pairs respectively. The standard tree-level Feynman amplitude for such a process can be written

$$i\mathcal{M} = \overline{u}(p_3)(-\frac{ig}{\sqrt{2}}\gamma^{\mu}P_L)v(p_4) \cdot \frac{-ig_{\mu\nu}}{(p_1+p_2)^2 - M_W^2} \cdot \overline{v}(p_2)(-\frac{ig}{\sqrt{2}}\gamma^{\nu}P_L)u(p_1), \tag{3.27}$$

with corresponding diagram

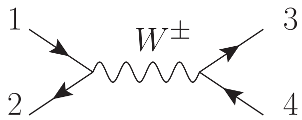

. (3.28)

We now apply the chirality-flow formalism to this process. Both the massless and massive cases will be contrasted with equivalent processes within QED and QCD.

3.1 The Massless Fermion Case

In the massless case, chirality and helicity are one-to-one, as $\alpha = 0$, and the external fermions carry a single definite chirality. The charged current vertex factor $C_R = 0$, meaning only left-chiral fermion flow can connect through the W boson. Any external flow carrying right-handed chirality flow contributes zero to the amplitude, without any algebraic manipulation.

Due to this there is an immediate difference as compared to an equivalent process in QED and QCD. Here all four possible left- and right-chiral combinations for the fermion lines would be possible, resulting in four distinct diagrams (2 possible combinations on each side $2 \cdot 2 = 4$):

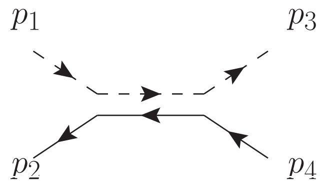

(3.29)

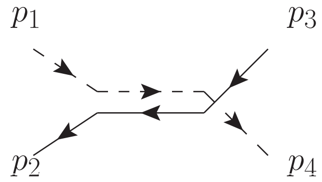

(3.30)

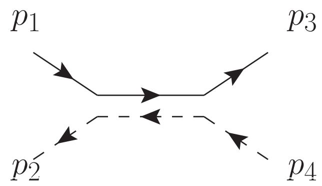

(3.31)

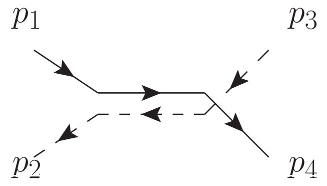

. (3.32)

In the charged current case, the W coupling eliminates every vertex except the one where both inward pointing fermion arrows carry left-handed chirality, meaning there is just a single diagram surviving:

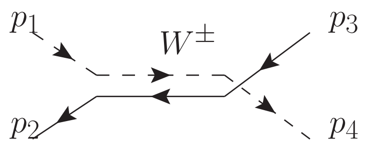

. (3.33)

We can then evaluate the amplitude from the diagram as

$$i\mathcal{M} \propto \frac{[p_1 p_4]\langle p_3 p_2\rangle}{q^2 - M_W^2}. \tag{3.34}$$

In the massless limit, the helicity configuration of every external fermion is entirely determined by the requirement that the amplitude is non-vanishing. As such, for every massless interaction involving a W vertex, the amount of diagrams reduces as the flow of chirality is locked in place on that branch.

3.2 The Massive Fermion Case

When fermion masses are included, helicity and chirality stop being one-to-one. The spinor for a massive fermion of definite helicity contains contributions from two chirality

Table 1: The 16 possible combinations of $p^\flat$ and q, marked with a checkmark if non-vanishing or a cross if vanishing

$[14]\langle 32\rangle$	$[p_1^\flat p_4^\flat]$	$[p_1^\flat q_4]$	$[q_1 p_4^\flat]$	$[q_1 q_4]$
$\langle p_3^\flat p_2^\flat\rangle$	✓	✓	✓	✗
$\langle p_3^\flat q_2\rangle$	✓	✓	✓	✗
$\langle q_3 p_2^\flat\rangle$	✓	✓	✓	✗
$\langle q_3 q_2\rangle$	✗	✗	✗	✗

components, $p^\flat$ and q (along with a prefactor depending on phase and $\sqrt{\alpha}$, see eqs. (2.17) and (2.18)). As such, two possible helicity states contribute from each particle, and one might naively assume that the total possible chirality-flow diagrams is $2^4 = 16$ for each of the four possible chirality-flow configurations, so 64 in total.

However, due to the definite chirality-flow imposed by the W, only the left-chiral components contribute, so this immediately reduces to 16 diagrams. Furthermore, recall from section 2.5 that each massive external spinor decomposes into two lightlike fourvectors, $p^\flat$ and q. This q acts as a reference vector which we can choose such that by antisymmetry we have $[qq] = 0$ and $\langle qq\rangle = 0$, so any diagram containing such components vanishes.

We choose the same reference vector q (where the axis corresponds to different spin directions) for all external particles, such that $q = q_1 = q_2 = q_3 = q_4$, and enumerate all possible spinor combinations in Table 1, indicating whether the brackets vanish or not. As Table 1 shows, 7 out of the 16 possible combinations vanish, leaving nine surviving diagrams. The disappearing configurations are those in which one of the flow lines contains two q. For equivalent processes in QED and QCD, the right-chiral components of these configurations would still contribute.

Worth noting is that the remaining nine configurations can largely be split into 3 families: One with no contribution from q, corresponding to the massless diagram, four with contributions from q in one of the flows, and four which carry contributions from q on both flows.

3.3 The Ultra-Relativistic Limit

In the ultra-relativistic limit, where fermion momenta satisfy $|\vec{p}| \gg m$ such that $p = p^\flat + \alpha q \to p^\flat$, the q components of all external spinors are suppressed. In other words, the nine massive diagrams collapse toward the single diagram in the first group, $[p_1^\flat p_4^\flat]\langle p_3^\flat p_2^\flat\rangle$, leading to the emergence of a *chirality lock* where the number of diagrams is limited in the massless case.

4 On-shell Decay of the W

We next examine the case where W appears as an on-shell external state. Here we first consider the case of an unspecified on-shell external boson decaying to a fermion-antifermion pair:

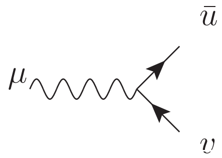

. (4.35)

In this case we need to consider the three polarization states, two transverse $\epsilon^{L,R}$ and one longitudinal ϵ^0 (Note that the longitudinal polarization only exists for massive bosons). This means we get 12 chirality-flow diagrams for decay (2 vertex types, 2 possible directions of flow, and 3 polarization states). The full amplitude receives a separate contribution from each of these polarization states, and in general all three must be evaluated and summed to obtain the complete result.

Now, assuming the decaying boson is a W, such that , $W^{\pm}(p_W) \rightarrow f(p_1)\overline{f}(p_2)$, we know that the left-chiral component must be connected to the anti-fermion, eliminating all diagrams where this is not the case. This cuts the total number of diagrams in half, reducing the amount to 6. It is worth noting however, that the longitudinal polarization is 0 for massless vector bosons, so the actual decrease in comparison to QED and QCD is 2 (from 8 to 6).

4.1 Transverse Polarization

As given in eq. 2.23 and eq. 2.24, the transverse polarization vectors are dependent on the spin direction. In the chirality-flow diagram for this process, the (close to) on-shell W attaches to the approximately massless fermion line through the vertex, and its polarization vector contributes a flow line such that we get the following diagrams for ϵ^{μ}_{L}, ϵ^{μ}_{R}:

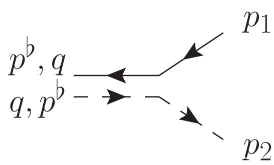

. (4.36)

We can then choose the reference vector to be one of the external fermion momenta, i.e. $q_W = p_1$ or $q_W = p_2$ (where p_1 and p_2 are the momenta of $\overline{u}$ and v respectively). In the first of these ϵ^L has q in the right bracket, which thus contracts to $\langle p_1 q_W \rangle = \langle q_W q_W \rangle$, which vanishes. It then follows that the contribution of the left-chirality vector is 0 by choice of spin direction. This leaves, the ϵ^- as the only contributing transverse polarization vector, as it is non-zero. Choosing $q_W = p_2$ reverses the roles. In either case, only one of the two contributes, effectively halving the amount of transverse diagrams.

4.2 The Longitudinal Polarization

Unlike the transverse modes, the longitudinal polarization vector ϵ^0, can't be made to vanish by choice of reference vector, as there will always be a non-vanishing element in the sum as seen in eq. 2.25. Therefore, the longitudinal polarization will always contribute to the amplitude. As seen in the diagram

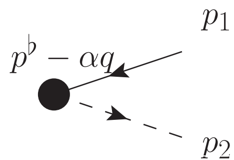

$$. \tag{4.37}$$

Choosing $q_W = p_1$, we end up with $\langle q_W p_W^\flat \rangle [p_W^\flat p_2]$ (non-bracket factors excluded), with the q_W term of the longitudinal polarization vanishing.

5 Extension to Higher Multiplicity

5.1 External Bosons on Fermion Lines

Consider extending the massless $f\overline{f} \to W^\pm \to f\overline{f}$ process by attaching additional external vector-bosons to one of the external fermion branches, such as a $2 \to 3$ process like

$$f(p_1) + \overline{f}(p_2) \to f'(p_3) + \overline{f}'(p_4) + \gamma(p_5)$$

where the photon is radiated from one of the external fermions.

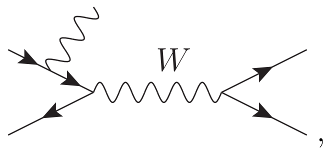

$$, \tag{5.38}$$

or

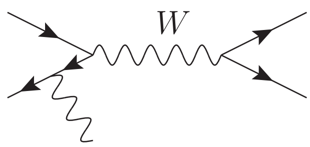

$$\tag{5.39}$$

etc.. The corresponding chirality-flow diagrams are:

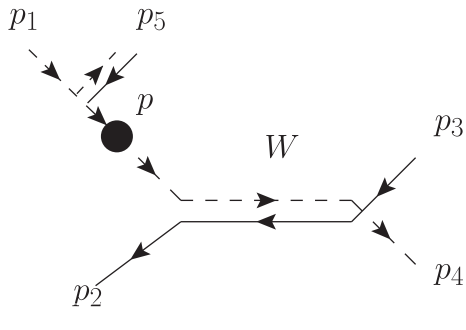

$$\tag{5.40}$$

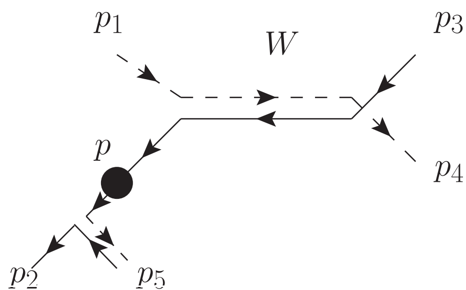

$$\tag{5.41}$$

Notably, it is immediately apparent that the W vertex fixes chirality along the fermion line, as was seen in section 3.1. The photon vertex, despite coupling to both chiralities, connects a dotted and an undotted index. However, since the chirality flow line is already determined by the W vertex, no new flow configurations are introduced. The number of non-vanishing chirality-flow diagrams for the massless case, therefore, remains unchanged.

The mechanism responsible for this also exists in QED and QCD, occurring due to how the massless fermion propagator works, but allows for four more cases. More explicitly, what it means is that once a fermion line is connected to a W-vertex, the chiralities are locked for the entire Feynman diagram, in the case of massless fermions and in the absence of non-Abelian gauge-boson-vertices.

5.2 W-Radiation

Consider a general diagram where a massless fermion emits an external W boson via the charged current vertex, changing flavour to a different internal massless fermion which then participates in an interaction vertex of arbitrary type, such as

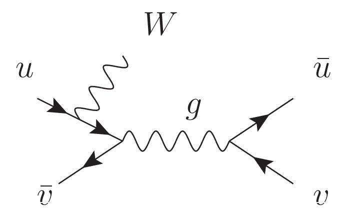

(5.42)

As seen in section 3.1 the presence of the W vertex immediately fixes the flow on the initial fermion line. The internal massless fermion propagator then carries a momentum dot in the chirality-flow language, which crosses the chirality type. The chirality arriving at the second vertex is then not a free variable, but is locked upstream by the W.

This has an important consequence, since, similarly to section 5.1, it means that any vertex connected to the fermion line via a chain of massless propagators originating from a W vertex inherits the constraints imposed there. A second vertex from the left will, in essence, behave as if the the chiral projection operator were present there too.

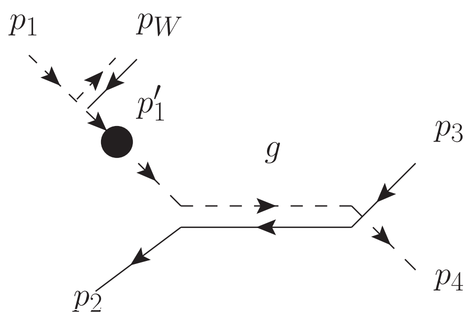

(5.43)

The number of surviving chirality-flow configurations for the locked line is, as such, always one, irrespective of the complexity of the remainder of the diagram. In other words, we completely eliminate a factor 4.

A further consequence of the structure originates from the internal propagator. The internal fermion momentum is expressed as a linear combination of the external momenta:

$$p_1' = p_1 - p_W. \tag{5.44}$$

This means that the momentum involving p_1' decomposes into brackets involving p_1 and p_W.

Decomposing the massive p_W as

$$p_W = p_W^\flat + \alpha q_W, \tag{5.45}$$

we get

$$p_1' = p_1 - p_W^\flat - \alpha q_W. \tag{5.46}$$

Choosing our reference vector to be $q_W = p_1$(meaning ϵ^R vanishes), for ϵ^L we write

$$\frac{i}{(p_1')^2}[p_1|\frac{|p_W^\flat]\langle q_W|}{\langle q_W p_W^\flat\rangle}((1-\alpha)|p_1\rangle[p_1| - |p_W^\flat\rangle[p_W^\flat|) = \frac{i}{(p_1')^2}\frac{[p_1 p_W^\flat]\langle p_1 p_W^\flat\rangle}{\langle p_1 p_W^\flat\rangle}[p_W^\flat|, \tag{5.47}$$

and for ϵ^0

$$\frac{i}{(p_1')^2}[p_1|\frac{|p_W^\flat]\langle p_W^\flat| - \alpha|q_W]\langle q_W|}{m_W\sqrt{2}}((1-\alpha)|p_1\rangle[p_1| - |p_W^\flat\rangle[p_W^\flat|) = \frac{i(1-\alpha)([p_1 p_W^\flat]\langle p_W^\flat p_1\rangle[p_1|}{(p_1')^2 m_W\sqrt{2}}. \tag{5.48}$$

Thus we see that for longitudinal polarization the momentum is effectively the same as for the external fermion.

Furthermore, if we look at the left polarized case seen in eq. (5.47), at the next vertex we end up with a boson propagator flow depending only on $p_W^\flat$ and p_2 . This cascades into the treatment of the external fermion pair on the opposite side of the boson propagator. Here we can choose reference vectors as $q_3 = p_W^\flat$ or $q_3 = p_2$, causing further brackets to vanish, which in case of massive fermions would reduce the number of nonzero terms even further to:

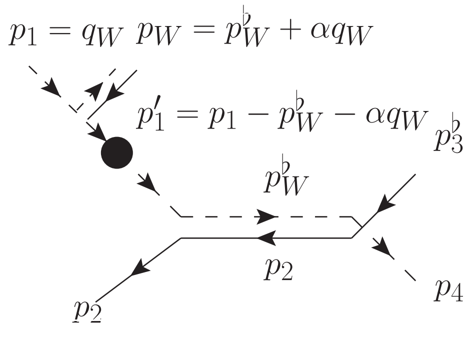

(5.49)

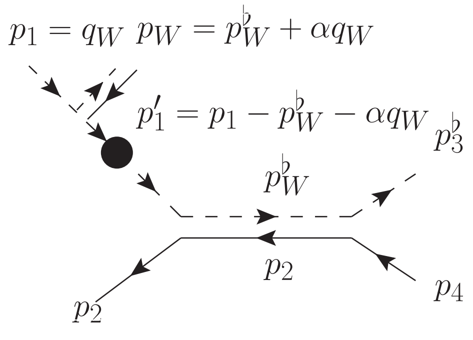

(5.50)

Note that the W can be radiated from any external leg, and that our choice of reference vector only affects the above case.

6 Results and Conclusion

The application of the chirality-flow formalism to charged current weak interactions has been investigated, with the aim of characterising the simplifications that the chiral nature of the W boson introduces, which were expected to reach beyond those found in QED and QCD. The results confirm this expectation and the simplifications made are both substantial and systematic across processes.

In the massless limit, the left-handed projection operator at every charged current vertex uniquely determines the number of contributing chirality flow diagram. This reduction follows not from cancellations but directly from the topology of the diagrams. In the massive fermion scattering case, this reduces the total amount of diagrams from 64 to 16, a number which can be further simplified, through choice of reference vector, to nine. The massless limit is here also recovered as $p = p^\flat + \alpha q \to p^\flat$.

We then extended this to the decay of an on-shell external W boson, showing that through the choice of reference vector the contribution of one transverse polarization vector can be eliminated, leaving only the opposite vector and the longitudinal polarization.

It was shown that when additional external bosons are attached to the fermion line, with the massless fermion propagator transmitting the fixed chirality between vertices, the chirality flow for the entire branch is set. A QCD or QED vertex connected to such a line is constrained by the weak vertex on the other end, not by its own Feynman rules.

These results confirm that the chirality-flow formalism is particularly well suited to the electroweak case, and that the chiral nature of the charged current interaction leads to simplifications in the investigated cases.

7 Outlook

There exists several natural venues for future work. The most obvious extension of the work presented in this thesis lies in non-Abelian three- or four-gauge-boson-vertices. Understanding whether and how the lock on chirality flow propagates through such vertices, as well as investigating which reference vector choices are most suitable, would be interesting.

Finally, the reference vector choices made in this thesis suggest that implementation into an event generator such as MadGraph may be practical.

Acknowledgements

I would like to thank my supervisor, Malin Sjödahl, for her continuous guidance, valuable feedback, and patience throughout the thesis process.

Acknowledgement of use of AI

During the writing of this thesis AI has been used for minor language improvements.

References

[1] Michael E. Peskin and Daniel V. Schroeder. *An introduction to quantum field theory (frontiers in physics)*. Westview Press Incorporated, 1995.

[2] Lance J. Dixon. “A brief introduction to modern amplitude methods”. In: *Journeys Through the Precision Frontier: Amplitudes for Colliders* (Sept. 2015), pp. 39–97. DOI: 10.1142/9789814678766_0002.

[3] Stephen J. Parke and T. R. Taylor. “Amplitude for an n gluon scattering”. In: *Physical Review Letters* 56.23 (June 1986), pp. 2459–2460. DOI: 10.1103/physrevlett.56.2459.

[4] Andrew Lifson, Christian Reuschle, and Malin Sjodahl. “The chirality-flow formalism”. In: *The European Physical Journal C* 80.11 (Oct. 2020). DOI: 10.1140/epjc/s10052-020-8260-8.

[5] Andrew Lifson, Malin Sjödahl, and Zenny Wettersten. “Automating scattering amplitudes with chirality flow”. In: *The European Physical Journal C* 82.6 (June 2022). DOI: 10.1140/epjc/s10052-022-10455-1.

[6] S. L. Glashow, J. Iliopoulos, and L. Maiani. “Weak interactions with lepton-hadron symmetry”. In: *Physical Review D* 2.7 (Oct. 1970), pp. 1285–1292. DOI: 10.1103/physrevd.2.1285.

[7] Michelangelo L. Mangano and Stephen J. Parke. “Multi-parton amplitudes in gauge theories”. In: *Physics Reports* 200.6 (Feb. 1991), pp. 301–367. DOI: 10.1016/0370-1573(91)90091-y.

[8] Joakim Alnefjord et al. “The chirality-flow formalism for the standard model”. In: *The European Physical Journal C* 81.4 (Apr. 2021). DOI: 10.1140/epjc/s10052-021-09055-2.

8 Appendix

A Tables for Chirality-flow

Table 2: Table showing chirality-flow diagrams for massive fixed-spin-axis fermions with corresponding Feynman diagrams and Bra-ket notation. Massless spinors are found by setting $\alpha = 0$

Species	Bra-Ket	Feynman Diagram	Chirality-flow
$u^+(p)$	$\begin{pmatrix} -e^{-i\phi}\sqrt{\alpha}\vert q] \\ \vert p^\flat\rangle \end{pmatrix}$	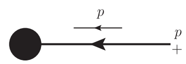	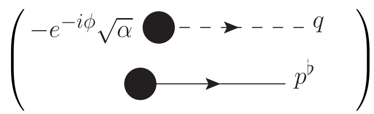
$u^-(p)$	$\begin{pmatrix} \vert p^\flat] \\ e^{i\phi}\sqrt{\alpha}\vert q\rangle \end{pmatrix}$	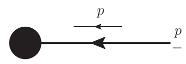	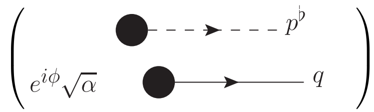
$\overline{u}^+(p)$	$([p^\flat\vert, -e^{i\phi}\sqrt{\alpha}\langle q\vert)$	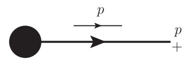	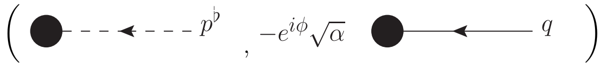
$\overline{u}^-(p)$	$(e^{-i\phi}\sqrt{\alpha}[q\vert, \langle p^\flat\vert)$	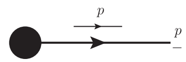	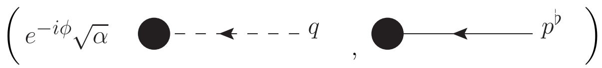
$v^+(p)$	$\begin{pmatrix} \vert p^\flat] \\ -e^{i\phi}\sqrt{\alpha}\vert q\rangle \end{pmatrix}$	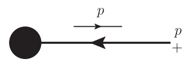	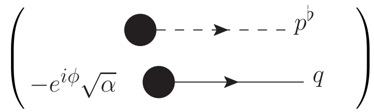
$v^-(p)$	$\begin{pmatrix} e^{-i\phi}\sqrt{\alpha}\vert q] \\ \vert p^\flat\rangle \end{pmatrix}$	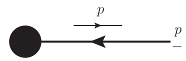	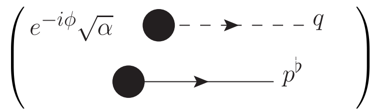
$\overline{v}^+(p)$	$(-e^{-i\phi}\sqrt{\alpha}[q\vert, \langle p^\flat\vert)$	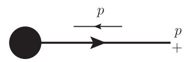	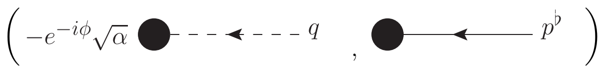
$\overline{v}^-(p)$	$([p^\flat\vert, e^{iq}\sqrt{\alpha}\langle q\vert)$	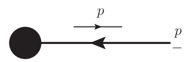	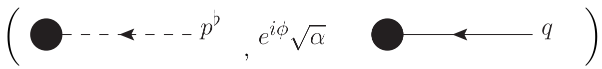

.